Chrysazin semiquinone radical anion

A theoretical study of the influence of the solvent on the electron spin resonance spectrum

Spanget-Larsen, Jens

Chrysazin semiquinone radical anion. A theoretical study of the influence of the solvent on the electron spin resonance spectrum.

Jens Spanget-Larsen

Department of Science and Environment, Roskilde University, Universitetsvej 1, DK-4000 Roskilde, Denmark.

ABSTRACT.

The strong influence of the solvent on the hyperfine coupling constants of the semiquinone radical anion derived from chrysazin (1,8-dihydroxy-9,10-anthraquinone) was investigated by theoretical calculations, using the polarizable continuum models IEFPCM and IPCM. The current implementation of the popular IEFPCM model does not describe the influence of specific interactions between solute and solvent molecules. This model thus requires incorporation of hydrogen-bonded solute-solvent clusters to approximate the situation in alcoholic and aqueous solvents. The results using the IPCM model suggest that it may be used as a tool to simulate the effect of rapidly changing formation and breaking of solute-solvent complexes by means of an average electrostatic reaction field at the position of the solute species, thus approximating the influence of specific effects within the polarizable continuum picture.

E-mail address: Spanget@ruc.dk (J. Spanget-Larsen)
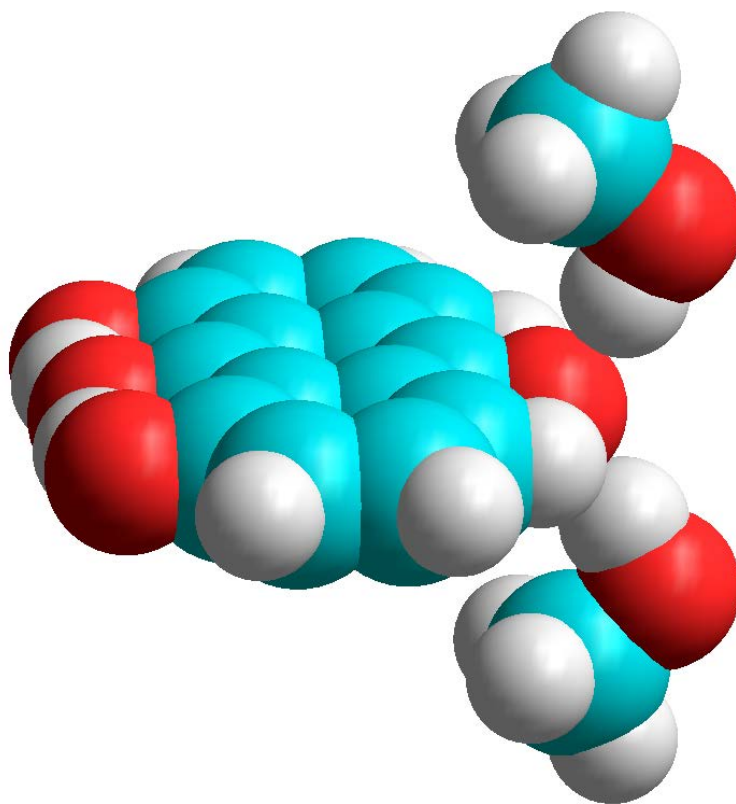
Graphical abstract

Highlights

- Hyperfine constants of chrysazin semiquinone in aprotic and protic media

- Theoretical computation of solvent effects on the hyperfine constants

- Calculations in the polarizable continuum solvation models IEFPCM and IPCM

- Combination of solvent cluster and polarizable continuum solvation models

1. Introduction

Semiquinone radical anions have been investigated extensively by electron spin resonance (ESR) spectroscopy, partly because of the importance of many of these radicals as intermediates in biological redox processes, and a wealth of experimental hyperfine data is available for this class of relatively stable radicals [1]. But the analysis of the observed ESR spectra is frequently complicated by a strong interaction with the solvent. The relative values of the hyperfine constants may thus be rearranged by the impact of the solvent, as observed for example for a number of benzosemiquinones, leading to conflicting assignments in the literature of the constants to distinct positions in the radicals [2-7].

An important example is the semiquinone radical anion $\mathbf{C}^{\cdot-}$ derived from chrysazin (1,8-dihydroxy-9,10-anthraquinone), see Scheme 1. Chrysazin is the redox active part of anthracycline antibiotics of the aclacinomycin type [8,9]. Divergent assignments of the proton hyperfine constants to distinct positions in $\mathbf{C}^{\cdot-}$ have been published [9-12], but Stegmann and associates [9] demonstrated that the discrepancy can be explained by the influence of the solvent. These authors performed a systematic study of the ESR spectra of $\mathbf{C}^{\cdot-}$ in mixtures of aprotic and protic solvents and subsequently applied the observed solvent dependence as an assignment criterion in their study of the semiquinones of the antitumor drug aclacinomycin A and 7-deoxyaklavinone [9].
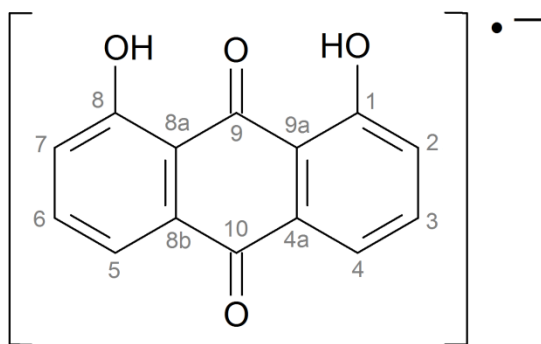
Scheme 1. Chrysazin semiquinone radical anion ($\mathbf{C}^{\cdot-}$) with atom numbering.

In the present investigation, the ability of modern theoretical solvation models to predict the hyperfine constants of $\mathbf{C}^{\cdot-}$ in liquid solution is investigated. Molecular dynamics simulation studies of the liquid state with explicit representation of hundreds or thousands of molecules are possible [13-17]. These studies allow the investigation of important thermal effects, but they are highly demanding in terms of theoretical knowhow and computational effort. We shall consider computationally more feasible static procedures with simulation of the influence of the solvent by Polarizable Continuum Models (PCM)

3

[15-25]. In particular, we shall explore applications of the Integral Equation Formalism Polarizable Continuum Model (IEFPCM) [21-23] and the Isodensity Polarizable Continuum Model (IPCM) [24,25]. As we shall show, the different philosophies behind the current implementations of the two models [26] lead to different performance characteristics.

2. Calculations

All quantum chemical calculations were performed with the GAUSSIAN16 software package [26], using unrestricted B3LYP [27,28] density functional theory (DFT) and the EPR-II basis set [29]. This basis has an enhanced *s* part and is optimized for the computation of hyperfine coupling constants by DFT methods (particularly B3LYP). Calculations were performed on the semiquinone in the gas phase and with inclusion of solvent effects by using the IEFPCM [23] and the IPCM [25] Self-Consistent Reaction Field (SCRF) models [19,26]. The IEFPCM calculations were performed with the GAUSSIAN16 default parameters, while input parameters IsoD and ε to the IPCM calculations were selected as described in Section 3.4. Calculations were also performed on C_{2v} symmetrical clusters with two methanol molecules in order to simulate the impact of the formation of hydrogen bonding with an alcoholic solvent (S1). All molecular geometries were optimized, except in the case of the IPCM model where the gas phase geometry was used (GAUSSIAN16 does not allow optimization of geometries with IPCM). Atomic charge distributions and spin populations were computed with the natural bond orbital (NBO) procedure [30]. Further information, including nuclear coordinates, molecular energies, isotropic Fermi contact couplings, spin dipole couplings, anisotropic spin dipole couplings, and NBO charges and spin populations are provided as Supplemental data, referred to in the ensuing text as S1 – S11.

3. Results and Discussion

3.1 Gas phase

The isotropic ^{1}H hyperfine coupling constants computed for the semiquinone $\mathbf{C^{\cdot-}}$ in the gas phase are listed in Table 1. Corresponding ^{13}C and [17]O constants are given in S3 and further details are provided in S5 with nuclear coordinates, NBO charges, and NBO spin populations. The predicted ordering of the methine proton constants is $|a_{3,6}| > |a_{2,7}| > |a_{4,5}|$ which is consistent with the assignments of the values measured in aprotic solvents like *N,N*-dimethylformamide (DMF) [9] and dimethylsulfoxide (DMSO)

4

[10], as ultimately determined by Stegmann and associates [9]. In aqueous and alcoholic media, $\mathbf{C}^{\cdot-}$ is affected by the formation of hydrogen bonds between solute and solvent. This is expected to affect in particular the exposed carbonyl oxygen at position 10, since the oxygen center at position 9 is screened by twofold intramolecular hydrogen bonds with the neigbouring hydroxyl groups. Adequate treatment of a solute species embedded in a close clustering of solvent molecules is a computational challenge. In order to simulate the impact of the formation of hydrogen bonds between O10 and alcoholic solvent molecules, calculations were performed on four different model clusters with methanol (MeOH) molecules. The geometry optimizations were restricted to C_{2v} symmetry, considering complexes with two MeOH species positioned either in the semiquinone plane or in positions perpendicular to this plane (S1). The most stable of the four investigated geometries is shown in Fig. 1; details are provided in S1 and S6. The optimized C_{2v} geometry is not at equilibrium (see S6); the complex should be considered as a simplified super-molecular model to approximate the impact of hydrogen bonding on the predicted hyperfine constants. As indicated in Table 1, the impact is strong, leading to the ordering $|a_{2,7}| > |a_{4,5}| > |a_{3,6}|$. This corresponds to a complete re-ordering of the relative magnitudes, consistent with the assignment of the ^{1}H constants measured in MeOH [9]. The ^{13}C and [17]O constants computed for the hydrogen-bonded cluster are given in S3 and S6, including also nuclear coordinates and NBO charges and spin populations. They indicate even more drastic rearrangements, particularly of the ^{13}C constants, with positive and negative shifts of several Gauss. Unfortunately, no experimental information seems to be available for these constants.

3.2 IEFPCM

This is one of the most popular solvation models and is the default SCRF solvation model in GAUSSIAN16 [26]. Generally, the PCM models provide a representation of the bulk of the solvent as a polarizable dielectric continuum. In the IEFPCM model, the solute molecule is contained in an empty cavity defined as a superposition of interlocked atomic spheres, using a continuous surface charge formalism [19,23]. It is likely that variation of the parameters of the model, such as the radii of the atomic spheres, would have a substantial influence on the predicted results, but this has not been attempted in the present work. IEFPCM calculations on $\mathbf{C}^{\cdot-}$ using the default parameters of GAUSSIAN16 were performed for the solvents tetrahydrofuran, methanol, *N,N*-dimethylformamide, dimethylsulfoxide, H_2O, formamide, and *N*-methylformamide-mixture [26]. The isotropic ^{1}H hyperfine constants predicted with all seven solvents are collected in S2. Results with *N,N*-dimethylformamide (DMF) and methanol

(MeOH) are given in Table 1, where they are compared with experimental values. For the abovementioned series of solvents, the dielectric constant (the ε parameter) ranges from 7.4257 to 108.94 (S2) [26]. Nevertheless, the computed hyperfine constants are quite similar, yielding in all cases the ordering $|a_{3,6}| > |a_{2,7}| > |a_{4,5}|$, similar to the gas phase prediction. The predicted ordering is consistent with the assignment of the constants measured in an aprotic solvent like DMF, but not with the assignment of those measured in MeOH (Table 1). Supplementary data for $\mathbf{C^{\cdot -}}$ in the solvents DMF and MeOH are provided in S3, S7, and S8, including ^{1}H, ^{13}C, and [17]O hyperfine data, nuclear coordinates, and NBO charges and spin populations.

3.3   Discreet-continuum model

The PCM cavity model rests on the assumption that interactions with individual solvent molecules do not substantially affect the electronic structure of the solute. But in case of specific interactions, such as hydrogen bonding, it may be necessary to add discreet solvent molecules to the cavity [19]. The ^{1}H results of a mixed discreet-continuum calculation on $\mathbf{C^{\cdot -}}$ are included in Table 1, column MeOH/cl. In this calculation, the formation of hydrogen bonds is approximated by the cluster model (Fig. 1), as discussed in the previous Subsection 3.1, and the influence of the bulk of a surrounding methanol solvent is represented by the IEFPCM model. The predicted ordering of the methine ^{1}H constants is now $|a_{2,7}| > |a_{4,5}| > |a_{3,6}|$, which is similar to the result of the corresponding cluster calculation in the gas phase (Table 1). The results are consistent with the assignment of the hyperfine constants measured in a strongly hydrogen-bonding solvent like methanol [9]. Supplementary data with all ^{1}H, ^{13}C, and [17]O hyperfine constants, nuclear coordinates, and NBO charges and spin populations are provided in S3 and S9.

3.4   IPCM

In this PCM model the boundary of the solute cavity is defined as an isodensity surface, that is, a surface of constant electron density. This surface is relaxed in the solvent reaction field and thus reflects the reactive shape of the molecule [24,25]. The IPCM model requires two input parameters, the isodensity value (IsoD) and the dielectric constant of the continuum. Different input parameters are appropriate for different solute-solvent systems. In a previous investigation on benzosemiquinones [7], calculations were performed with IsoD values between 0.001 and 0.003. The present calculations were carried out with an isodensity of 0.0015 and with dielectric constants ε ranging from 1 to 30. The dependence of the

computed hyperfine constants on ε is shown in Figs. 2, 3, and 4. In general, increasing the ε value above unity leads to large shifts, particularly in the case of [13]C (Fig. 3). Experimental values for the ^{13}C and [17]O hyperfine constants of $\mathbf{C^{\cdot-}}$ do not seem to be available (an investigation would probably be rewarding).

The computed ^{1}H hyperfine constants as a function of ε are shown in Fig. 2. Values computed with $\varepsilon =$ 1, 1.5, 2 and 30 are listed in Table 2, together with experimental values measured in DMSO, DMF, EtOH/H_2O and MeOH. Additional information including data for ^{13}C and [17]O are given in S4, S10, and S11. The computed ^{1}H constants are essentially linearly related to $1 - \varepsilon^{-0.7}$, as shown in Fig. 5a, providing a convenient representation of the results on a scale from zero ($\varepsilon = 1$) to unity ($\varepsilon = \infty$). Fig. 5b shows the measured ^{1}H constants as a function of the volume fraction ϕ_{MeOH} in a series of mixtures of DMF and MeOH [9]. These results enable a continuous representation of the transition from the aprotic solvent DMF ($\phi_{MeOH} = 0$) to the protic solvent MeOH ($\phi_{MeOH} = 1$). Comparison of the curves in Figs. 5a and 5b demonstrates that the theoretical prediction reproduces important experimental trends.

Large solvent sensitivities are predicted for the methine protons, *positive* for H3,6 and *negative* for H2,7 and H4,5, in excellent consistency with the experimental ones (Table 2). Hence, drastic shifts in the relative magnitudes of the constants are predicted and observed:

(1)   For $\varepsilon < 1.5$ the computed ordering of the methine ^{1}H constants is $|a_{3,6}| > |a_{2,7}| > |a_{4,5}|$. This is consistent with the assignments of the constants measured in aprotic solvents like DMSO and DMF (Table 2).

(2)   For ε values in the region $2 - 3$ the predicted ordering is $|a_{2,7}| > |a_{3,6}| > |a_{4,5}|$, as observed in 3/2 (v/v) EtOH/H_2O (Table 2) and in DMF/MeOH with ϕ_{MeOH} in the range $0.2 - 0.4$ (Fig. 5b).

(3)   Finally, for $\varepsilon > 5$ the ordering is $|a_{2,7}| > |a_{4,5}| > |a_{3,6}|$ as observed in pure MeOH.

In this context, ε is considered as an adjustable model parameter, not necessarily reflecting the actual dielectric constant of the solvent medium. But it is apparent that an increase of ε value in the calculation parallels the influence of increasing polarity and protic character of the solvent on the measured constants. Taken at face value, the IPCM approximates the effect of a protic solvent by a suitable choice of the parameters IsoD and ε, without an explicit representation of hydrogen-bonded complexes between

solute and solvent molecules. This supports the assumption that the rapidly changing formation and breaking of complexes can be considered as giving rise to an average electrostatic reaction field at the position of the solute species [7]. It is noteworthy that semiempirical procedures with simple electrostatic effective solvent field (ESF) models account adequately for the hyperfine data for benzosemiquinones in alcoholic and aqueous solvents [5,6].

4. Conclusions

IEFPCM [23] as implemented in GAUSSIAN [26] is one of the most popular and effective SCRF solvation models. It has been parameterized for a large number of solvents and allows geometry optimization in the SCRF. But it is not directly applicable to strongly hydrogen-bonded systems, like the chrysazin semiquinone radical anion ($C^{\cdot-}$) in alcoholic and aqueous solvents, where the IEFPCM model requires explicit incorporation of hydrogen-bonded solute-solvent clusters [19]. The IPCM model [25] is based on a different strategy. According to the present results for $C^{\cdot-}$, the model may be parametrized to incorporate in an average manner the influence of rapidly changing formation and breaking of hydrogen-bonded complexes between solute and solvent. IPCM thus describes within the SCRF framework the evolution of the solvent effect in a series of mixtures of aprotic and protic solvents, judging from the results for $C^{\cdot-}$ shown in Fig. 5. Whether IPCM is generally successful, with similarly promising results for other solute-solvent systems, must await the results of further investigations. The possibility to simulate the influence of a protic solvent without explicit consideration of discreet solute-solvent complexes would mean a great simplification of obvious practical significance. But the approach is likely to fail when stable complexes are formed and when solvation leads to substantial changes in solute molecular geometry.

Competing interests
The author declares no competing interests.

Appendix A. Supplementary data
Supplementary data to this article can be found online at . . .

Table 1

Chrysazin semiquinone radical anion ($\mathbf{C}^{\cdot-}$). Isotropic ^{1}H hyperfine coupling constants a_H [Gauss = 10^{-4} Tesla] predicted in the gas phase and with the IEFPCM solvation model. Experimental values included for comparison. Additional results including computed ^{13}C and [17]O constants are provided as Supplemental data (S2, S3, S7–S9).

	Gas phase		IEFPCM[a,b]			Experimental[b,c]	
	-	cl.[d]	DMF	MeOH	MeOH/cl.[d]	DMF	MeOH
H1,8	–0.35	–0.28	–0.35	–0.35	–0.29	–0.20	–0.18
H2,7	–1.13	–1.91	–1.27	–1.27	–2.04	–1.12	–1.80
H3,6	–1.59	–0.79	–1.37	–1.37	–0.61	–1.46	–0.80
H4,5	–0.18	–1.24	–0.59	–0.58	–1.58	–0.57	–1.40

[a] Integral Equation Formalism Polarizable Continuum Model.
[b] Solvent: DMF = N,N-dimethylformamide, MeOH = methanol.
[c] Experimental values measured at 253 K [9].
[d] Cluster with two methanol molecules, see main text.

Table 2

Chrysazin semiquinone radical anion ($\mathbf{C}^{\cdot-}$). Isotropic ^{1}H hyperfine coupling constants a_H [Gauss = 10^{-4} Tesla] and their solvent sensitivities a_H' predicted with the IPCM model and corresponding values measured in different solvents. Additional results including computed ^{13}C and [17]O constants are provided as Supplemental data (S4, S10, S11).

	IPCM[a]					Experimental				
	$\varepsilon = 1.0$	$\varepsilon = 1.5$	$\varepsilon = 2.0$	$\varepsilon = 30$	a_H'[b]	DMSO[c]	DMF[d]	EtOH/H_2O[e]	MeOH[f]	a_H'[g]
H1,8	–0.35	–0.34	–0.33	–0.30	*+0.02*	–0.20	–0.20	–0.20	–0.18	*+0.01*
H2,7	–1.13	–1.31	–1.42	–1.89	*–0.43*	–1.06	–1.12	–1.68	–1.80	*–0.44*
H3,6	–1.59	–1.38	–1.24	–0.68	*+0.51*	–1.51	–1.46	–1.27	–0.80	*+0.49*
H4,5	–0.18	–0.31	–0.65	–1.33	*–0.72*	–0.52	–0.57	–0.92	–1.40	*–0.63*

[a] Isodensity Polarizable Continuum Model. Isodensity = 0.0015, ε = dielectric constant.
[b] Theoretical solvent sensitivity a_H' = $[da_H/d\varepsilon]_1$, i.e., the derivative of the predicted value with respect to ε, taken for $\varepsilon = 1$.
[c] Solvent dimethylsulfoxide [10,12], according to the presently accepted assignment [9,12].
[d] Solvent N,N-dimethylformamide [9].
[e] Solvent 3/2 (v/v) ethanol-water [12].
[f] Solvent methanol [9].
[g] Experimental solvent sensitivity a_H' = $da_H/d(\phi_{MeOH})_{0.5}$, i.e., the derivative of the measured value with respect to the volume fraction ϕ_{MeOH} of a DMF/MeOH solvent mixture, estimated for $\phi_{MeOH} = 0.5$ [9].

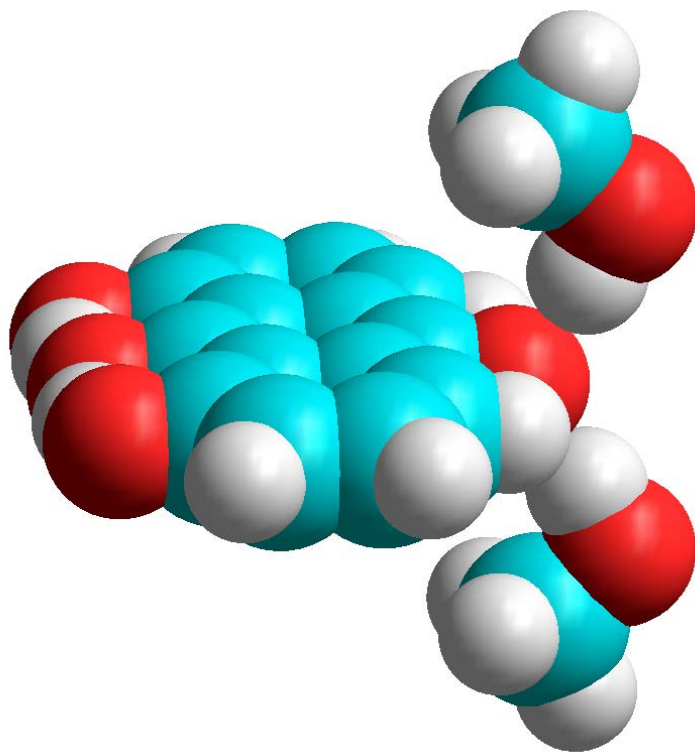**Fig. 1.** Model complex of chrysazin semiquinone (**C·⁻**) with two methanol molecules. See main text.
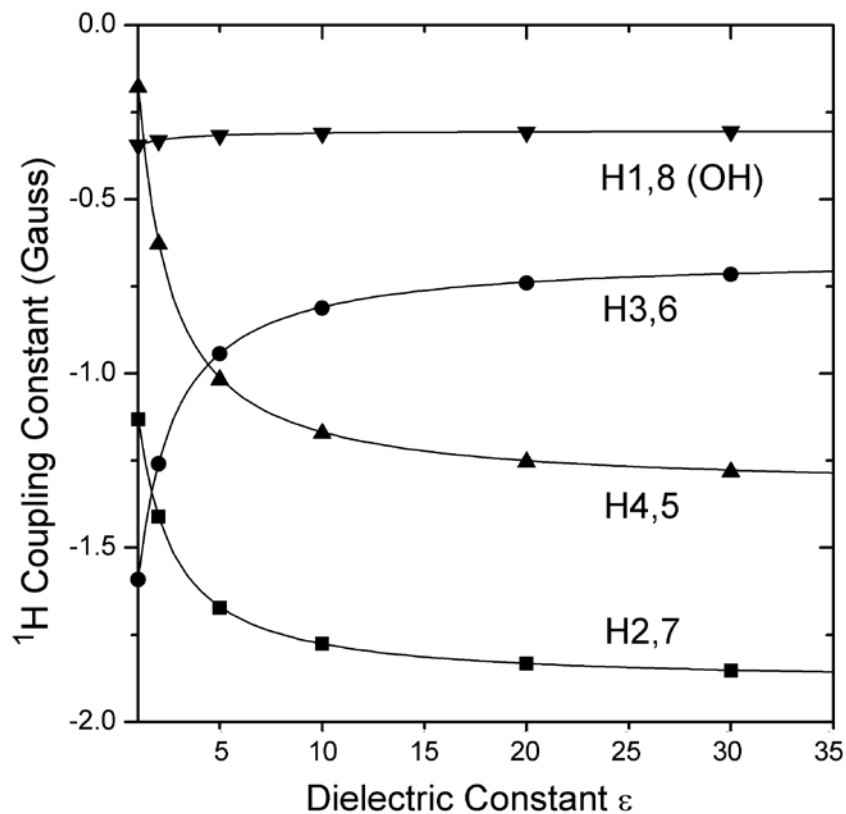
Fig. 2. [1]H hyperfine constants of chrysazin semiquinone ($\mathbf{C^{\cdot-}}$) computed with IPCM as a function of the dielectric constant of the solvent. The curves in this and the following two figures show logistic dose response functions $y = A_2 + (A_1 - A_2)/(1 + (x/x_0)^p)$ fitted to the computed points [31].
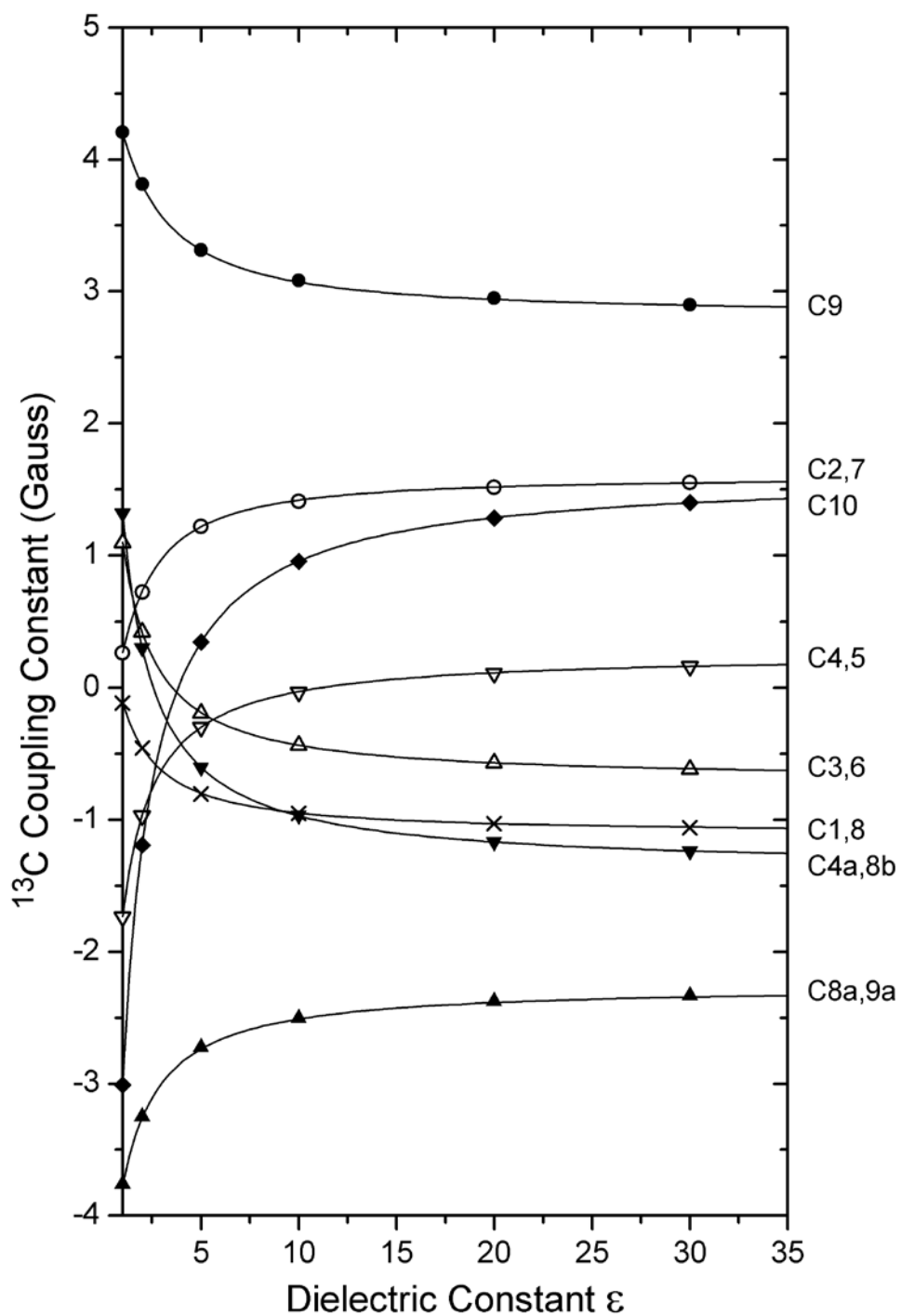
Fig. 3. [13]C hyperfine constants of chrysazin semiquinone (**C·⁻**) computed with IPCM as a function of the dielectric constant of the solvent.
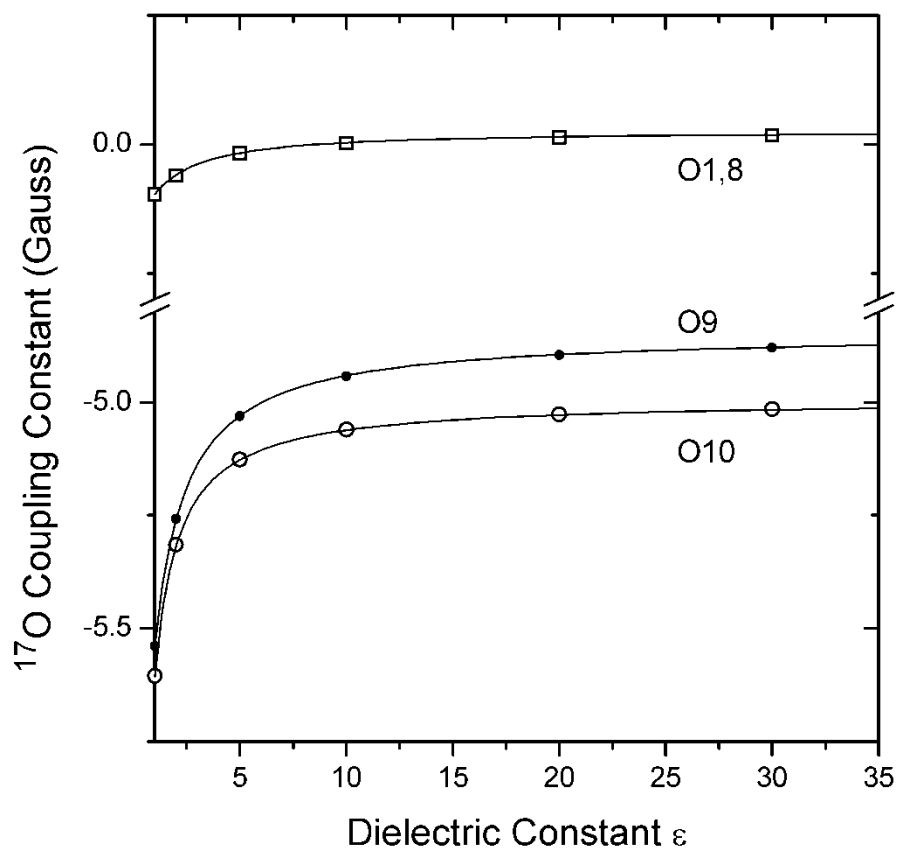
Fig 4. ^{17}O hyperfine constants of chrysazin semiquinone ($\mathbf{C}^{\cdot-}$) computed with IPCM as a function of the dielectric constant of the solvent.
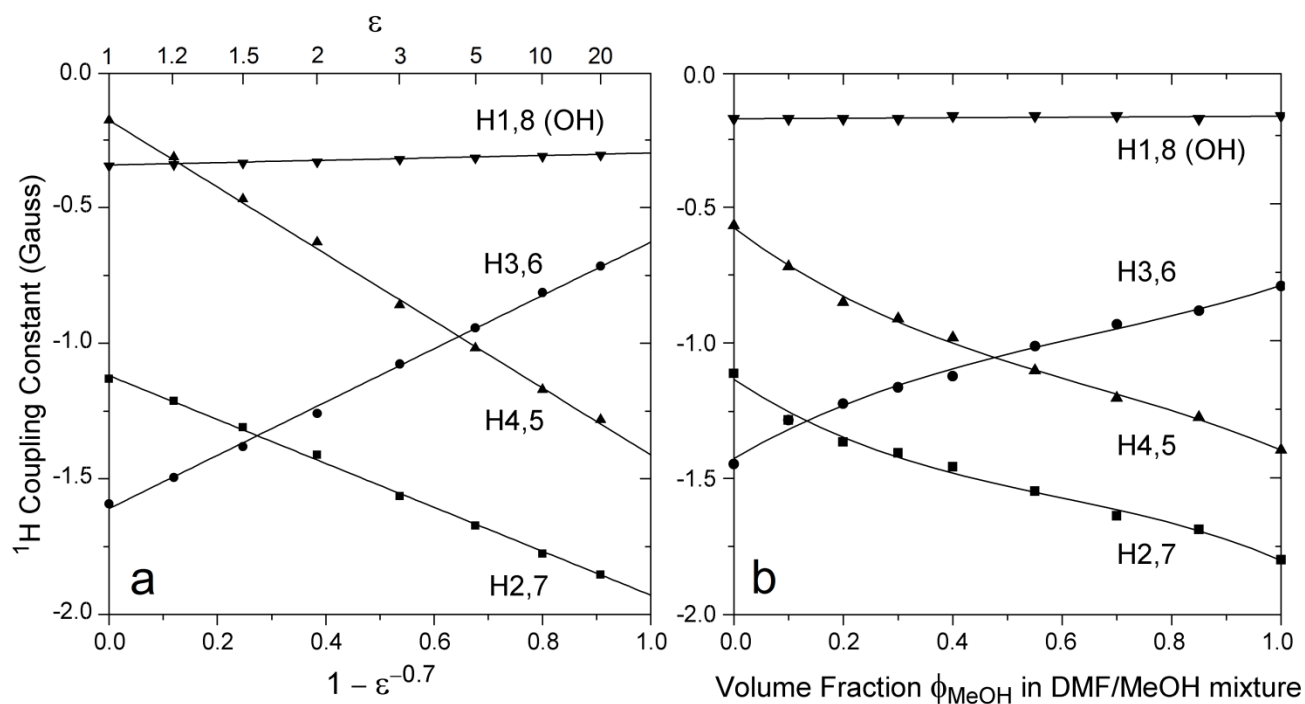
Fig 5. **(a)** [1]H hyperfine constants of chrysazin semiquinone ($\mathbf{C^{\cdot-}}$) computed with IPCM as a function of $1 - \varepsilon^{-0.7}$, where ε is the dielectric constant of the solvent. **(b)** [1]H hyperfine constants measured in mixtures of *N,N*-dimethylformamide (DMF) and methanol (MeOH) as a function of ϕ_{MeOH}, the volume fraction of methanol. Adapted with permission from Ref. [9] (copyright © 1991 by John Wiley & Sons, Ltd).

References

1   J.A. Pedersen, Handbook of EPR Spectra from Quinones and Quinols, CRC Press, Boca Raton, FL, 1985 (eBook 2018).

2   J.A. Pedersen, Assignment of the h.f.s. constants of 1,4-benzosemiquinones by additivity rules. The free rotation of *t*-butyl groups, Mol. Phys. 28 (1974) 1031-1035.

3   J. Spanget-Larsen, J.A. Pedersen, Solvent sensitivities of the Hyperfine Constants of Methyl and *t*-Butyl-Substituted 1,4-benzosemiquinones, J. Magn. Reson. 18 (1975) 383-389.

4   J.A. Pedersen, J. Spanget-Larsen, The strong influence of the solvent on the spin distribution in 1,2-benzosemiquinones. Chem. Phys. Letters 35 (1975) 41-44.

5   J. Spanget-Larsen, INDO Calculations with Inclusion of an Effective Solvent Field. Application to Benzosemiquinones, Theoret. Chim. Acta 47 (1978) 315-328.

6   J. Spanget-Larsen, Assignment of the Hyperfine Constants of the 1,2-Benzosemiquinone Radical Anion, Int. J. Quantum Chem. 18 (1980) 365-367.

7   M. Langgård, J. Spanget-Larsen, The strong influence of the solvent on the electron spin resonance spectra of semiquinone radical anions. I. A theoretical investigation of the hyperfine constants of 1,2- and 1,4-benzosemiquinone by using density functional theory and polarizable continuum solvation models, J. Mol. Struct. (Theochem) 431 (1998) 173-180.

8   B.R. J. Abdella, J. Fisher, A Chemical perspective on the Anthracycline Antitumor Antibiotics, Environ. Health Perspect. 64 (1985) 3-18.

9   Th. Jülich, H.B. Stegmann, K. Krohn, A. Eickhoff, EPR and ENDOR Investigations of Chrysazin and Aclacinomycin A Semiquinones, Magn. Reson. Chem. 29 (1991) 178-183.

10   J. Gendell, W.R. Miller, Jr., G.K. Fraenkel, Electron Spin Resonance Studies of Hydroxysemiquinone Radicals. Hydrogen-Deuterium Isotope Effects in Intramolecular Hydrogen Bonds, J. Amer. Chem. Soc. 91 (1969) 4369-4380.

11   D. Lunney, J. Bailes, J.D. Memory, Solvent Effects in the Electron Resonance Spectra of Some Hydroxyanthrasemiquinones, J. Chem. Phys. 53 (1970) 3387-3388.

12   J.A. Pedersen, R.H. Thomson, EPR study of hydroxyanthrasemiquinones. Assignment of hyperfine structure by additivity, J. Magn. Reson. 43 (1981) 373-386.

13   K. Bux, S.T. Moin, Solvation of cholesterol in different solvents: a molecular dynamics simulation study, Phys. Chem. Chem. Phys. 22 (2020) 1154-1167.

14   A. Jindal, S. Vasudevan, Geometry of OH···O interactions in the liquid state of linear alcohols from *ab initio* molecular dynamics simulations, Phys. Chem. Chem. Phys. 22 (2020) 6690-6697.

15   C.J. Cramer, D.G. Truhlar, Implicit Solvation Models: Equilibria, Structure, Spectra, and Dynamics, Chem. Rev. 99 (1999) 2161-2200.

16   M.A. Gonçalves, L.S. Santos, D.M. Prata, F.C. Peixoto, E.F.F. da Cunha, T.C. Ramalho, Optimal wavelet signal compression as an efficient alternative to investigate molecular dynamics simulations: application to thermal and solvent effects of MRI probes, Theor. Chem. Acc. 136 (2017) 15.

17   M.A. Gonçalves, L.S. Santos, F.C. Peixoto, T.C. Ramalho, NMR relaxation and relaxivity parameters of MRI probes revealed by optimal wavelet signal compression of molecular dynamics simulations, Int. J. Quantum Chem. 119 (2019) e25896.

18   J. Tomasi, B. Mennucci, R. Cammi, Quantum Mechanical Continuum Solvation Models, Chem. Rev. 105 (2005) 2999-3093.

19   J.B. Foresman, Æ. Frisch, Exploring chemistry with electronic structure methods, Third Edition, Gaussian, Inc., Wallingford CT, 2015. Chapter 5, Modelling Chemistry in Solution.

20   I. Ciofini, Use of Continuum Models in Magnetic Resonance Calculations, in: M. Kaupp, M. Bühl, V.G. Malkin (Eds.), Calculation of NMR and EPR Parameters. Theory and Applications, Wiley-VCH, Weinheim, 2004, Chapter 12, pp. 191-208.

21   S. Miertuš, E. Scrocco, J. Tomasi, Electrostatic interaction of a solute with a continuum. A direct utilizaion of AB initio molecular potentials for the prevision of solvent effects, Chem. Phys. 55 (1981) 117-129.

22   J. Tomasi, M. Persico, Molecular Interactions in Solution: An Overview of Methods Based on Continuous Distributions of the Solvent, Chem. Rev. 94 (1994) 2027-2094.

23   G. Scalmani, M.J. Frisch, Continuous surface charge polarizable continuum models of solvation. I. General formalism, J. Chem. Phys. 132 (2010) 114110.

24   K.B. Wiberg, P.R. Rablen, D.J. Rush, T.A. Keith, Amides. 3. Experimental and Theoretical Studies of the Effect of the Medium on the Rotational Barriers for N,N-Dimethylformamide and N,N-Dimethylacetamide, J. Am. Chem. Soc. 117 (1995) 4261-4270.

25   J.B. Foresman, T.A. Keith, K.B. Wiberg, J. Snoonian, and M.J. Frisch, Solvent Effects 5. The Influence of Cavity Shape, Truncation of Electrostatics, and Electron Correlation on ab initio Reaction Field Calculations, J. Phys. Chem. 100 (1996) 16098-16104.

26   M.J. Frisch, G.W. Trucks, H.B. Schlegel, G.E. Scuseria, M.A. Robb, J.R. Cheeseman, G. Scalmani, V. Barone, G.A. Petersson, H. Nakatsuji, X. Li, M. Caricato, A.V. Marenich, J. Bloino, B.G. Janesko, R. Gomperts, B. Mennucci, H.P. Hratchian, J.V. Ortiz, A.F. Izmaylov, J.L. Sonnenberg, D. Williams-Young, F. Ding, F. Lipparini, F. Egidi, J. Goings, B. Peng, A. Petrone, T. Henderson, D. Ranasinghe, V.G. Zakrzewski, J. Gao, N. Rega, G. Zheng, W. Liang, M. Hada, M. Ehara, K. Toyota, R. Fukuda, J. Hasegawa, M. Ishida, T. Nakajima, Y. Honda, O. Kitao, H. Nakai, T. Vreven, K. Throssell, J.A. Montgomery, Jr., J.E. Peralta, F. Ogliaro, M.J. Bearpark, J. J. Heyd, E.N. Brothers, K.N. Kudin, V.N. Staroverov, T.A. Keith, R. Kobayashi, J. Normand, K. Raghavachari, A.P. Rendell, J.C. Burant, S.S. Iyengar, J. Tomasi, M. Cossi, J.M. Millam, M. Klene, C. Adamo, R. Cammi, J. W. Ochterski, R.L. Martin, K. Morokuma, O. Farkas, J.B. Foresman, D.J. Fox, Gaussian16, Revision A.03, Gaussian, Inc., Wallingford CT, 2016.

27   A.D. Becke, Density-functional thermochemistry. III. The role of exact exchange, J. Chem. Phys. 98 (1993) 5648-5652.

28   C. Lee, W. Yang, R.G. Parr, Development of the Colle-Salvetti correlation-energy formula into a functional of the electron density, Phys. Rev. B 37 (1988) 785-789.

29   V. Barone, Structure, Magnetic Properties and Reactivities of Open-Shell Species from Density Functional and Self-Consistent Hybrid Methods, in: Recent Advances in Density Functional Methods, Vol. 1, Part I, D. P. Chong (Ed.), World Scientific Publ. Co., Singapore, 1995, pp. 287-334.

30   A.E. Reed, R.B. Weinstock, F. Weinhold, Natural-population analysis, J. Chem. Phys. 83 (1985) 735-746.

31   OriginLab Corporation, Northampton, MA 01060, USA. Logistic Dose Response Function. https://www.originlab.com/doc/LabTalk/ref/Logistic-func (accessed 20 May 2020).